

# DEUTSCHES ELEKTRONEN - SYNCHROTRON

DESY 93-063  
May 1993



## Fast Simulation of Longitudinal Hadron Shower Profiles in the ZEUS Calorimeter

A. F. Zarnecki

*Institute of Experimental Physics, Warsaw University, Poland*

ISSN 0418-9833

NOTKESTRASSE 85 · D - 2000 HAMBURG 52

**DESY behält sich alle Rechte für den Fall der Schutzrechtserteilung und für die wirtschaftliche Verwertung der in diesem Bericht enthaltenen Informationen vor.**

**DESY reserves all rights for commercial use of information included in this report, especially in case of filing application for or grant of patents.**

To be sure that your preprints are promptly included in the  
**HIGH ENERGY PHYSICS INDEX,**  
send them to (if possible by air mail):

**DESY**  
Bibliothek  
Notkestraße 85  
W-2000 Hamburg 52  
Germany

**DESY-IfH**  
Bibliothek  
Platanenallee 6  
D-1615 Zeuthen  
Germany

# Fast Simulation of Longitudinal Hadron Shower Profiles in the ZEUS Calorimeter

A.F.Żarnecki

Institute of Experimental Physics, Warsaw University

## Abstract

An algorithm for fast simulation of hadronic showers in the uranium-scintillator calorimeter is presented. The program is based on an analysis of the WA78 calorimeter test data. Through fluctuations of the mean shower profile the energy deposits in the calorimeter modules and the energy correlations between the modules are well reproduced. The program was prepared to study effects of longitudinal energy leakage in the ZEUS experiment.

## 1 Introduction

In high energy accelerator experiments calorimetry becomes more and more important. An interesting solution for optimizing energy measurements in terms of resolution and cost has been put forward by two experiments ZEUS [1] and H1 [2], built to study high energy  $e\pi$  scattering at the electron-proton storage ring HERA. The external iron yoke and muon absorber, surrounding the main components of the detector, is instrumented in such a way as to allow a complementary energy measurement for showers leaking out of the central, high resolution hadron calorimeter.

In case of the ZEUS experiment the main calorimeter is a sampling calorimeter (CAL) made of depleted uranium and scintillator, with depth of 4 to 7 interaction lengths,  $\lambda_{int}$ , followed by an iron backing calorimeter (BAC), made out of 8 to 11, 7.3 cm thick iron plates interleaved with aluminium proportional tubes. The depth of the CAL is such, that for 90% of hadronic showers at least 95% energy containment is obtained (within HERA energies) [3]. The energy resolution of the CAL, obtained for fully contained hadronic showers is about  $\frac{8\%}{\sqrt{E}}$  [4], while that of the BAC is about  $\frac{10\%}{\sqrt{E}}$  [5]. The test results, obtained in an exposure of the prototype calorimeter system to hadron beams at the CERN-SPS, show that the BAC can be used either to select a high resolution sample of events (fully contained in the CAL), or to correct for leakage by adding the measured signal [6]. The advantage of the latter approach is that with only slightly worse energy resolution all events can be used in the analysis.

Test results, however, can not be directly applied to predict the role of BAC for HERA physics. This can only be done by studying Monte Carlo simulated events passed through the detector. To study the role of BAC in the measurement of multiparticle hadron jets in the ZEUS detector, hundreds of thousands of events have to be simulated over the whole kinematic range accessible at HERA. This is only possible with a fast detector simulation

program based on a parametrization of hadronic showers. The program described in this note provides a fast simulation of hadronic showers and is based on a parameterization of the WA78 calorimeter test data [7]. Special emphasis was put on the description of the shower tail to account properly for the possible energy leakage. Only simulation of the longitudinal shower profile was considered, as the WA78 calorimeter provided no information on lateral energy distribution. The other data available are also not detailed enough, as to allow simultaneous parametrization of longitudinal and lateral shower development. The parametrization of the mean lateral shower profile, for hadronic cascades in a uranium-scintillator calorimeter, can be found in [8].

## 2 Description of the mean hadron shower profile

The WA78 calorimeter consisted of two sections: a uranium section with 48 plates of depleted uranium and 48 scintillator plates grouped into 12 modules, and an iron part with 52 elements in 13 modules [7], as shown in fig. 1. The depth of one uranium module was  $0.45 \lambda_{int}$ , and that of the iron module  $0.62 \lambda_{int}$ , resulting in the total depth of about  $13.5 \lambda_{int}$ . The calorimeter was exposed to hadron beams of energy ranging from 5 to 210 GeV.

Following the approach suggested by Bock [9], the mean hadron shower profile can be used to choose the analytical formula for the description of individual showers. In the case of the WA78 calorimeter the mean energy distribution is known very well, as the longitudinal information is very detailed (25 modules). However, in order to fit an analytical formula to the energy profile, the formula has to be integrated over the modules. This turns out to be a problem if many fits have to be performed, and the integration can not be done analytically. The solution is to analyse the integrated energy distribution

$$I(x) = \int_x^{\infty} dy s(y) \quad (1)$$

where:  $s(x) = \frac{1}{E} \frac{dE}{dx}$  is the normalized energy distribution profile  
 $x$  is the longitudinal position in the calorimeter, in units of  $\lambda_{int}$

The values of  $I(x)$  are determined in discrete points – at the module edges – and the fitted function has only to be evaluated at this points. Figure 2 shows the mean integrated energy distribution for 210 GeV hadrons. The boundary conditions for  $I(x)$ ,  $I(0)=1$  and  $I(\infty)=0$ , replace the normalization of the function  $s(x)$ .

The distribution obtained from the data is integrated over the vertex position. It is possible to obtain the actual shower profile from the measured distribution using the following two assumptions:

- the vertices of the showers are distributed according to an exponential dependence:

$$\rho(v) = \alpha \cdot e^{-\alpha v} \quad (2)$$

- the shower shape is independent of the vertex position, that is:

$$s(x) = \int_0^x dv \cdot s_0(x-v)\rho(v); \quad (3)$$

where  $s_0(x)$  is the mean shower profile measured from the vertex.

Then the integrated shower profile, as measured from the vertex can be expressed as follows:

$$I_0(x) = I(x) + \frac{1}{\alpha} \cdot \frac{dI(x)}{dx}, \quad (4)$$

where  $\alpha$  is defined by equation 2. The value extracted from the vertex distribution for hadron cascades in the WA78 calorimeter is [10]

$$\alpha = 0.84 \pm 0.01. \quad (5)$$

The  $I_0(x)$  profiles obtained for this value of  $\alpha$ , for hadron events at different energies, are shown in fig. 3.

It was found that the tail of the integrated profile can be very well described by the following formula:

$$I_0(x) \sim \exp(-b \cdot x^p), \quad (6)$$

where  $b$  and  $p$  are energy dependent parameters. About 30% of the energy is deposited very close to the vertex and is taken into account by adding to eq. (6) a short-range contribution. As the longitudinal segmentation of the detector was not sufficient to determine this short-range component, it was assumed to be of the form typical for integrated electromagnetic cascades,

$$E(t) = \int_t^\infty dz \cdot \frac{z^3}{96} \cdot \exp(-\frac{z}{2}), \quad (7)$$

where  $t$  (and  $z$ ) is the distance from the shower vertex in radiation lengths. The constant integer value, assumed in the formula for the power of  $z$ , allows an analytical integration.

The full formula describing the mean shower profile, including both the tail and the short-range terms can now be written as follows:

$$I_0(x) = w \cdot E(t) + (1 - w) \cdot \exp(-b \cdot x^p), \quad (8)$$

where  $w$  is the fraction of energy deposited by the short-range component of the shower  $-E(t)$ . The results of the fit for  $I_0(x)$ , at different hadron energies, are represented by the solid lines in fig. 3. As can be seen the shower profile is well described by eq. (8).

### 3 Simulation of shower fluctuations

The approach to fast simulation of hadronic showers adopted in the program is based on the assumption that every single cascade can be described by the same functional form (8) as the mean shower profile. The parameters  $w$ ,  $b$  and  $p$  can however fluctuate from event to event. Also the position of the shower vertex  $v$  varies according to eq. (2). There are thus four parameters describing the shape of each individual shower. The distribution of these parameters was determined by fitting the shower profile of each event. In addition to the four shape parameters, the total shower energy  $E$  and the longitudinal leakage fraction  $\epsilon$  (important for late starting showers) were fitted as well.

As can be seen in fig. 4 the distribution of the vertices obtained from the fits follows the expected exponential dependence. Also the total energy distribution has the expected gaussian shape (see fig. 5). The distribution of the short-range component fraction,  $w$ , as shown in fig. 6a, has a more complicated form. In about 20% of events the fraction

$w$  is consistent with zero and one term is sufficient to describe the shower. For the remaining events, with  $w > 0$ , the  $-\ln(w)$  distribution can be well approximated by a gamma distribution, as shown in fig. 6b.

The only nonnegligible correlation between the fitted parameters is observed for parameters  $b$  and  $p$ , as shown in fig. 7. This correlation can be taken into account by introducing two new, uncorrelated variables, both being functions of  $b$  and  $p$ . Two parameters were chosen, describing the longitudinal energy distribution in the long-range shower component: the mean depth  $M$  and  $RMS/\sqrt{M}$ , where  $RMS$  is the dispersion of this distribution. As shown in fig. 8, these parameters are uncorrelated and can be used for simulation as two independent random variables. Their respective distributions happen to be well described by analytical forms. After transformation of the generated  $M$  and  $RMS/\sqrt{M}$  variables, the correlation between  $b$  and  $p$  is well reproduced, as shown in fig. 9.

To simulate a shower initiated by a hadron of given energy  $E$ , four parameters describing the shape, have to be generated according to their respective distributions: the vertex position  $v$ , the fraction of the short-range component  $w$ , and the mean depth  $M$  and  $RMS/\sqrt{M}$  of the long-range shower component. From fits performed at five different beam energies, from 20 to 210 GeV, it was found that the parameters of these distributions depend linearly on  $\ln(E)$ . This is shown in fig. 10, where the most probable values of variables  $-\ln(w)$ ,  $M$  and  $RMS/\sqrt{M}$  are plotted as a function of energy. The simulation of showers at different energies was based on the parameters interpolated to 100 GeV and their slope in  $\ln(E)$ . The parametrisation is numerically stable for energies greater than 2 GeV.

In the fast simulation program no attempt is made to generate energy deposits in individual active layers of the calorimeter. The response is generated for readout sections of the calorimeter, consisting of many passive and active layers, and the corresponding energy deposits are smeared to reproduce the measured energy resolution. In this analysis it was assumed that the dispersion of the response distribution is given by

$$\sigma = \text{const} \cdot \sqrt{< E >}, \quad (9)$$

where  $< E >$  is the mean calorimeter response, equal to the deposited energy. The response  $E$  was generated using a gamma distribution,

$$\rho(E) = \frac{B^P}{\Gamma(P)} \cdot E^{P-1} \cdot e^{-B \cdot E}, \quad (10)$$

where:  $P = \frac{\sigma^2}{< E >^2}$  and

$$B = \frac{P}{< E >} \quad \text{are the parameters of the gamma distribution.}$$

For  $\frac{\sigma}{< E >} \ll 1$  this is equivalent to a gaussian distribution. The advantage of this approach is that for wider distributions the response of the detector is always positive ( $\rho(E) \equiv 0$  for  $E \leq 0$ ) and is applicable even for  $\sigma \geq < E >$ . As for gaussian distributions, the sum of gamma-distributed random variables has a gamma distribution with,

$$\sigma^2 = \sum_i \sigma_i^2 \quad \text{and}$$

$$< E > = \sum_i < E_i >. \quad (11)$$

This relation is necessary if the energy resolution of the calorimeter is not to depend on the energy sharing between modules.

In addition, for all calorimeter modules, small gaussian smearing of the response was included, describing an energy independent noise.

## 4 Comparison with data

Since not all of the showers can be well described by the functional form appropriate for the mean profile, the agreement between data and the results of the simulation can be improved by some tuning of the final parameters of the fit. It was found that an increase of the generated longitudinal shower spread  $RMS/\sqrt{M}$  by 15% gives the best agreement with data. It may well be that a fit of 6 parameters to 24 energy deposits results in a smoothing of the shower profile and the information on some fluctuations is lost.

The comparison between the data and the results of simulation for some of the WA78 calorimeter modules is shown in fig. 11, for 20 and 210 GeV hadrons. As can be seen the response of a single modules is fairly well reproduced. The simulation reproduces very well the energy distribution in the whole uranium part of the calorimeter ( $5.45 \lambda_{int}$ ), as shown in fig. 12.

The description of the hadronic showers based on the WA78 data has been used to simulate the response of the forward ZEUS calorimeters test set-up [4,6], consisting of the high resolution, uranium-scintillator calorimeter (FCAL), 7.1  $\lambda_{int}$  deep, and an iron backing calorimeter (BAC), 4.9  $\lambda_{int}$  deep.

The simulation reproduces well the energy distribution in all sections of FCAL and in the whole calorimeter. This is shown in fig. 13, for 100 GeV hadron data. Also the correlation between signals from the so called HAC1 and HAC2 sections of the calorimeter are described very well, as can be seen in fig. 14.

The assumed logarithmic energy dependence of the simulation parameters reproduces well the evolution of the cascade development. Figure 15 shows the mean fraction of energy, measured in the last section of the uranium calorimeter - HAC2, as a function of energy. Simulation describes accurately the energy leakages into HAC2 observed in the test data.

The program can also describe well the response of the BAC prototype standing behind the FCAL (fig. 16). However, the detector parameters have to be tuned, as BAC is not a compensating calorimeter and the response to the shower tail is lower than to the short-range shower component. In fig. 17 the correlation of the energy measured in the FCAL prototype and that measured in BAC is shown for test data and for simulation. After tuning of the unknown detector parameters good agreement is obtained.

## 5 Conclusions

The WA78 data have been used to describe in detail the longitudinal profiles of hadronic showers in a large energy range. The results have been used to simulate the hadronic showers expected in the ZEUS calorimeter. Good agreement was found with the test data, both for the energy distributions in single calorimeter modules and for the energy correlations between modules. The program reproduces properly the FCAL-BAC correlation as well. The program is very fast, in one second of IBM-9000 CPU time about 4000

showers of 100 GeV hadrons can be generated, whereas full simulation of a 100 GeV hadron shower within the GEANT package [11] takes about 30 seconds. The program was successfully used for simulating the influence of the longitudinal energy leakage on the performance of the ZEUS detector [12].

## Acknowledgements

I would like to thank the members of the ZEUS collaboration, in particular from the Calorimeter (FCAL) and Backing (BAC) Groups for possibility of using their test data. Special thanks are due to H.Abramowicz, for many useful discussions and her help in preparing this paper.

## References

- [1] ZEUS, a Detector for HERA, Letter of Intent, DESY, June 1985.  
The ZEUS Detector, Technical Proposal, DESY, March 1986.  
The ZEUS Detector, Status Report 1989, DESY, March 1989.
- [2] Technical Proposal for the H1 Detector, DESY 1986.  
Technical Progress Report, H1 Detector, DESY 1987.
- [3] J.Krüger, DESY 90-163.
- [4] U.Behrens, et al., Nucl. Instr. and Meth. A289(1990)115.
- [5] H.Abramowicz, et al., ZEUS Note 90-099.
- [6] H.Abramowicz, et al., Nucl. Instr. and Meth. A313(1992)126.
- [7] M.G.Catanesi, et al., Nucl. Instr. and Meth. A253(1987)222.
- [8] F.Barreiro et al., Nucl. Instr. and Meth. A392(1990)259.
- [9] R.K.Bock et al., Nucl. Instr. and Meth. 186(1981)533.
- [10] J.Krüger, ZEUS Note 86-019.
- [11] R.Brun et al., CERN-DD/EE/84-1.
- [12] A. F. Zarnecki, et al., Proc. of the HERA Workshop, Hamburg 1991,  
Ed. W. Buchmüller i G. Ingelman (DESY Hamburg, 1992) Vol.1, p.115.

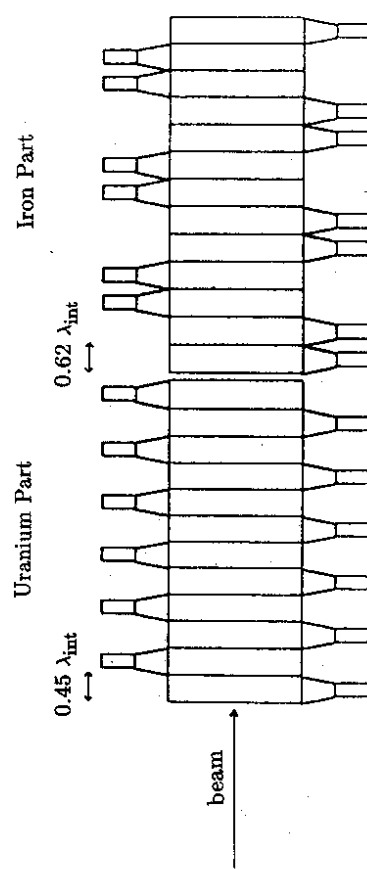


Figure 1: Schematic view of the WA78 calorimeter.

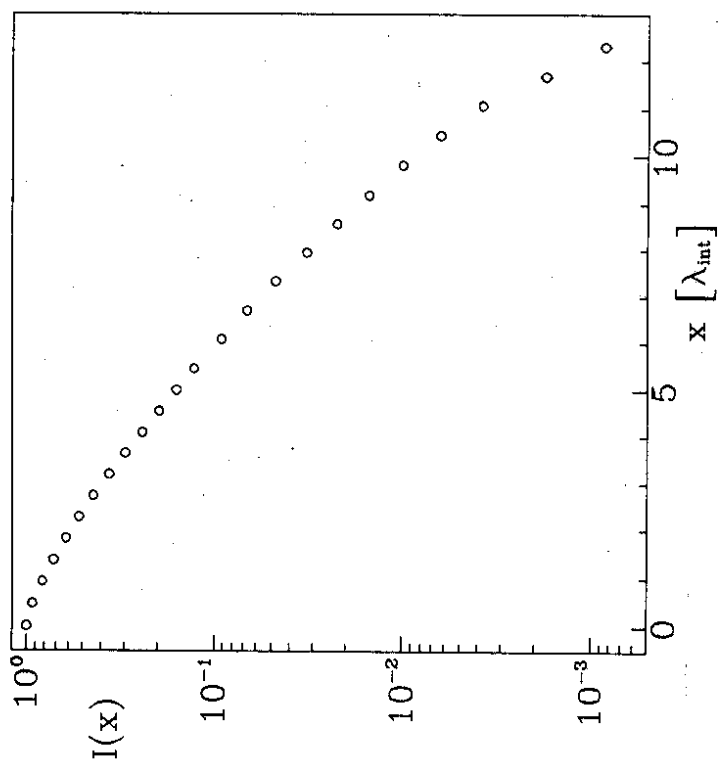


Figure 2: The fraction of the total shower energy -  $I$ , deposited at the distance greater than  $x$  from the face of the calorimeter, for 210 GeV hadron events.

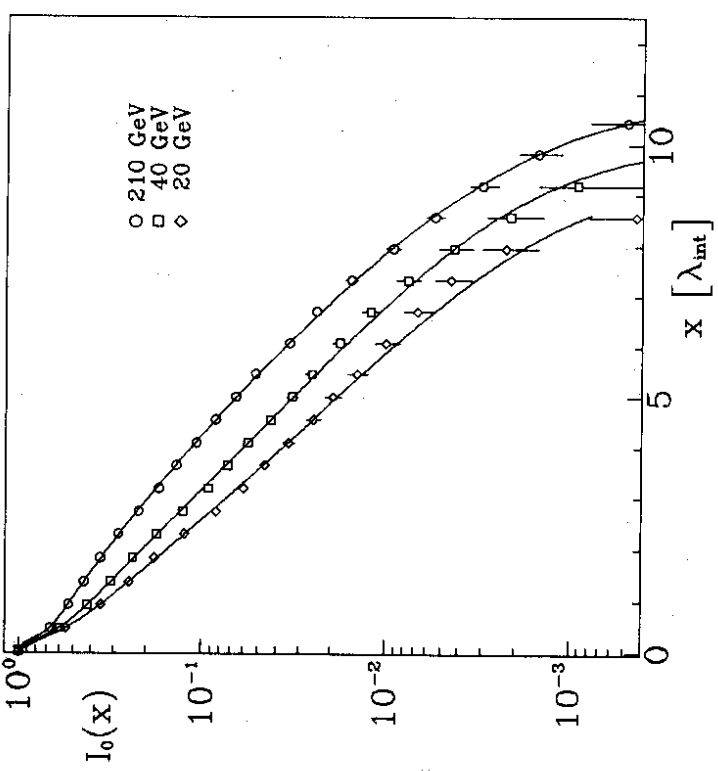


Figure 3: The fraction of the total shower energy -  $I_0$ , deposited at the distance greater than  $x$  from the shower vertex, for hadron events at different energies, as indicated on the plot. The solid lines are the fit results for the function chosen to describe mean shower profiles.

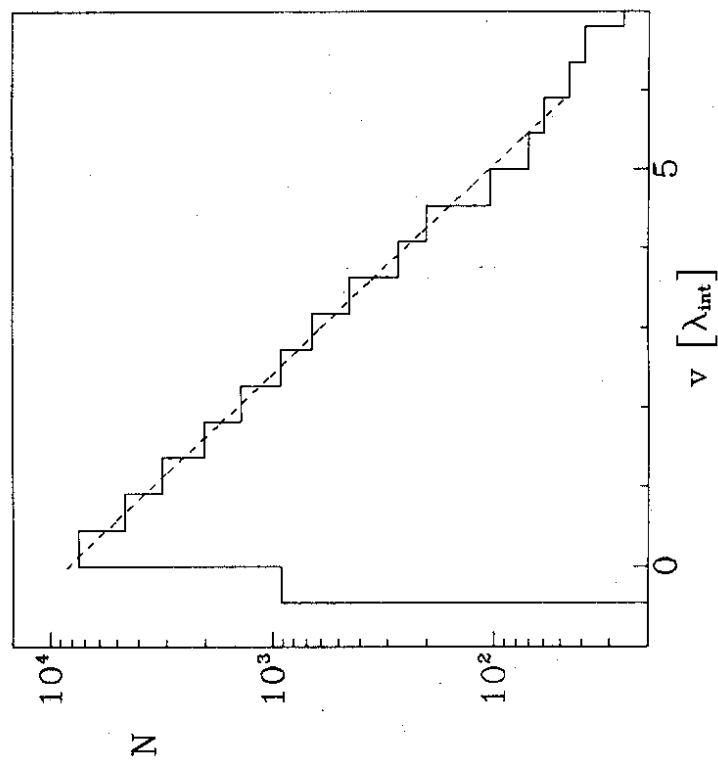


Figure 4: The distribution of the shower vertex position -  $v$ , as obtained from the shower profile fit to 210 GeV hadronic events. The dashed line is the result of the fit of an exponential function.

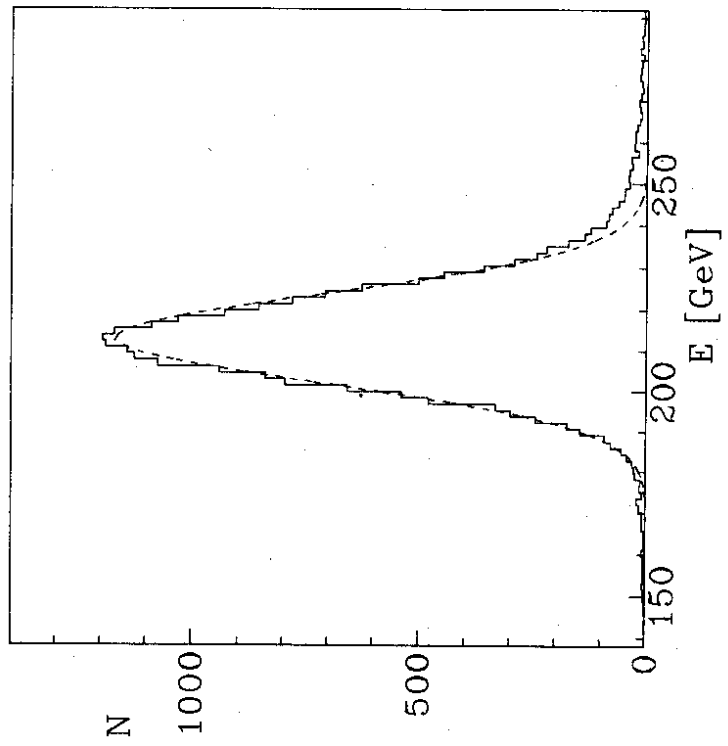


Figure 5: The distribution of the total energy  $E$ , as obtained from the shower profile fit to 210 GeV hadronic events. The dashed line is the result of the fit of a gaussian distribution, within  $\pm 2\sigma$ .

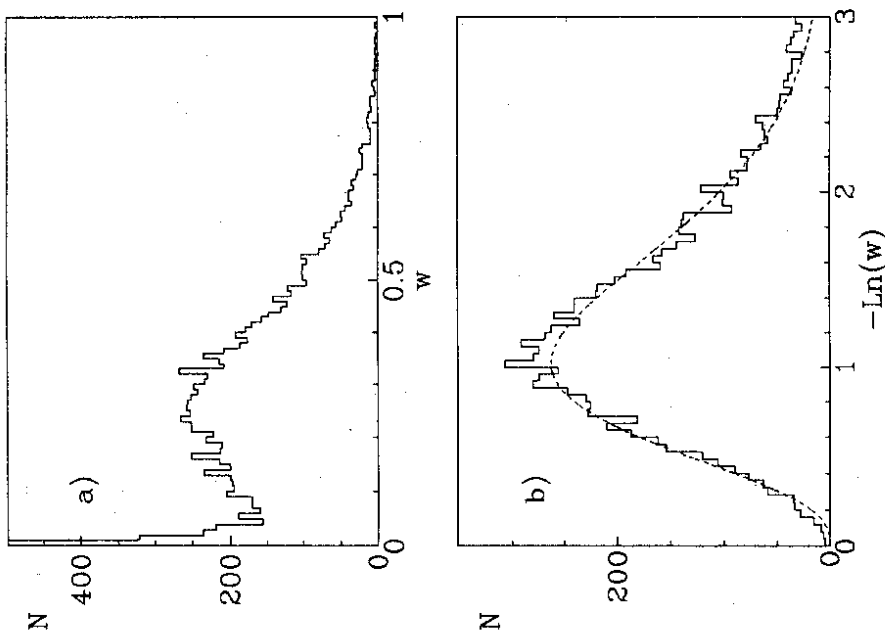


Figure 6: The distribution of the energy fraction carried by the short-range shower component  $-w$  (a), and the distribution of  $-\ln(w)$  (b), as obtained from the shower profile fit to 210 GeV hadronic events. The dashed line on figure (b) is the result of the fit of a gamma distribution.

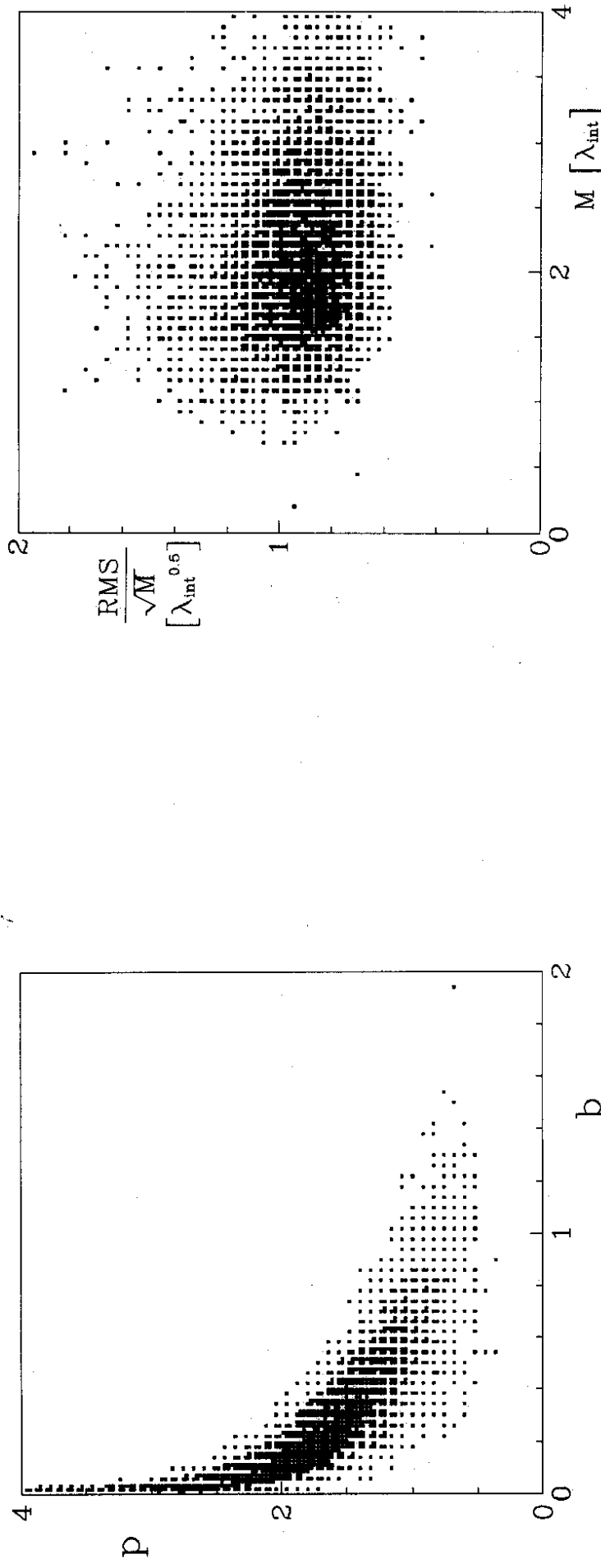


Figure 7: Correlation between the parameters  $p$  and  $b$ , describing the shape of the long-range shower component, as obtained from the shower profile fit to 210 GeV hadronic events.

Figure 8: Correlation between the dispersion of the long-range shower component  $RMS/\sqrt{M}$ , and the mean deposit depth  $M$ , as obtained from the shower profile fit to 210 GeV hadronic events.

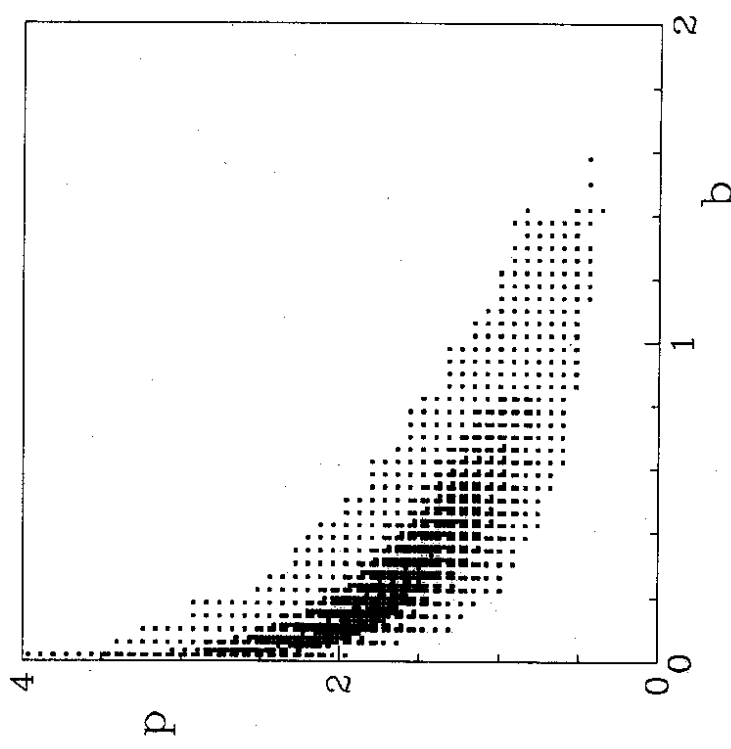


Figure 9: Correlation between the parameters  $p$  and  $b$ , describing the shape of the long-range shower component, obtained from the independent generation of variables  $M$  and  $RMS/\sqrt{M}$ .

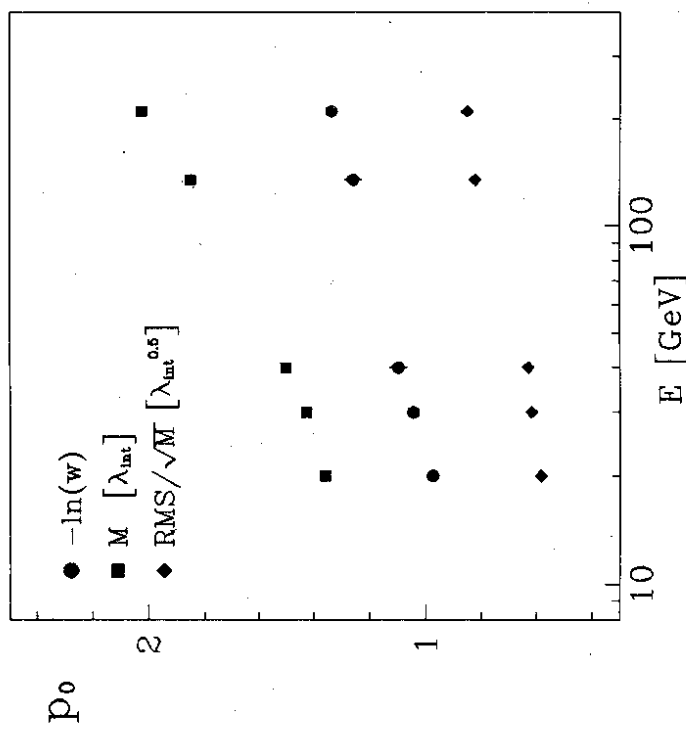


Figure 10: The energy dependence of the most probable parameter value  $p_0$  (position of the distribution maximum), for three selected parameters describing hadron shower development, as indicated on the plot.

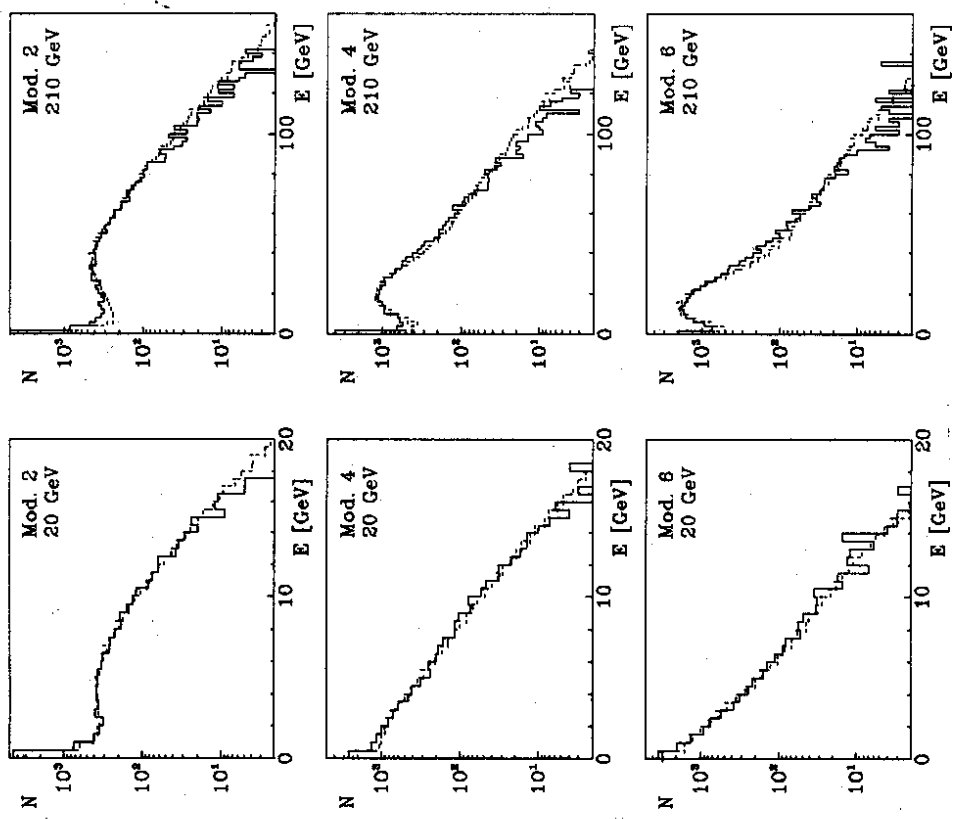


Figure 11: The distribution of energy  $E$  measured in selected modules of WA78 calorimeter (solid line), compared with simulation results (dashed line), for hadron energies 20 and 210 GeV.

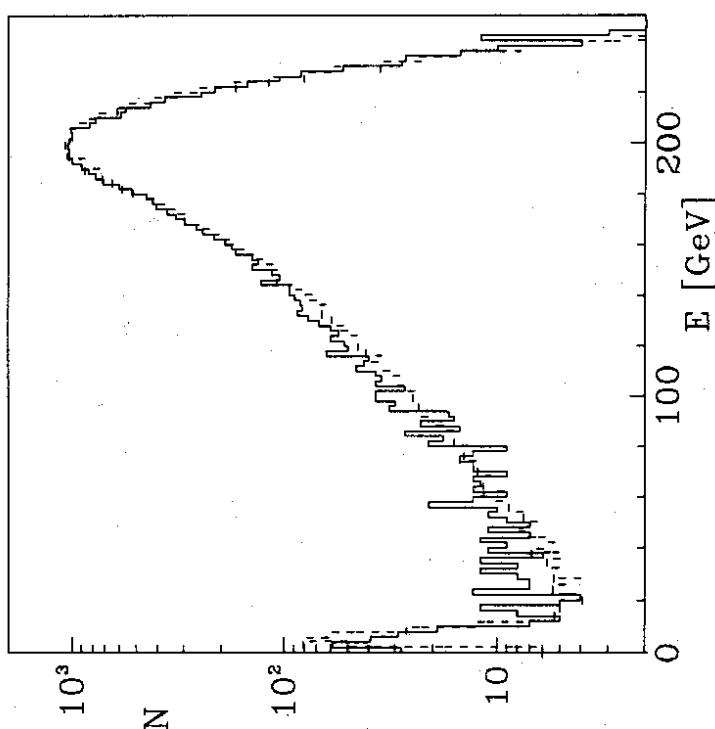


Figure 12: The distribution of energy  $E$  measured in the uranium part of WA78 calorimeter for 210 GeV hadron events (solid line), compared with simulation results (dashed line).

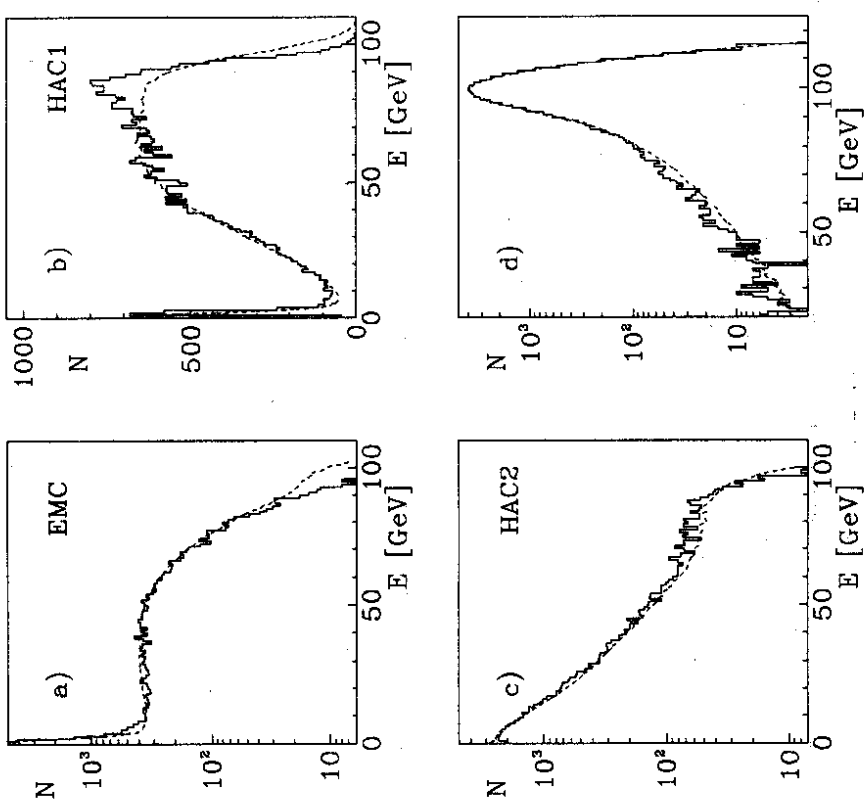


Figure 13: The distribution of energy  $E$  measured in separate sections of the FCAL prototype (a-c) and in the whole calorimeter (d), for 100 GeV hadron events (solid line), compared with simulation results (dashed line).

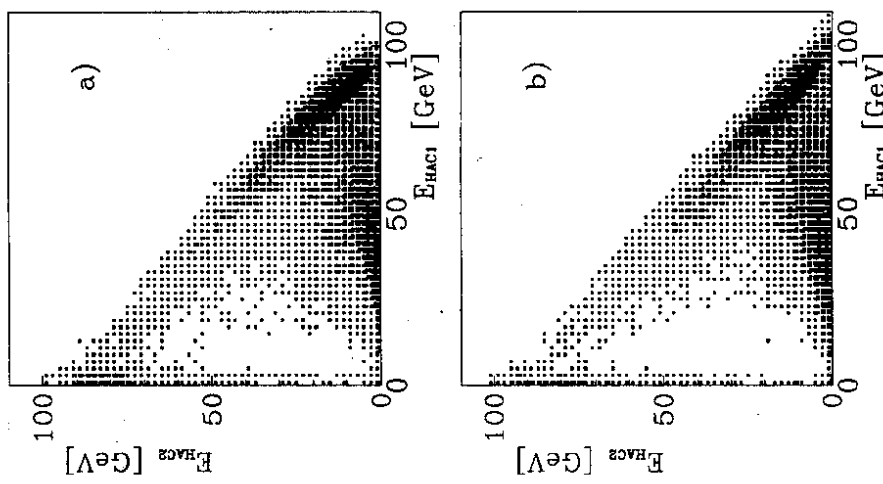


Figure 14: Correlation between the energy measured in the HAC2 section of FCAL -  $E_{HAC2}$  and the energy measured in the HAC1 section -  $E_{HAC1}$ , for 100 GeV hadron events as obtained from the test data (a) and from simulation (b).

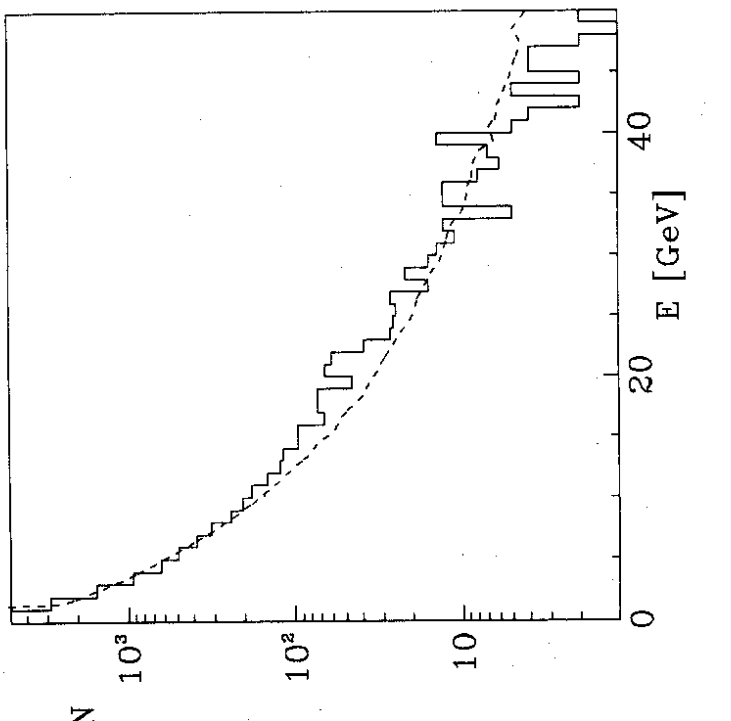


Figure 16: The distribution of energy  $E$  measured for 100 GeV hadron events in the BAC prototype standing behind FCAL (solid line), compared with simulation results (dashed line).

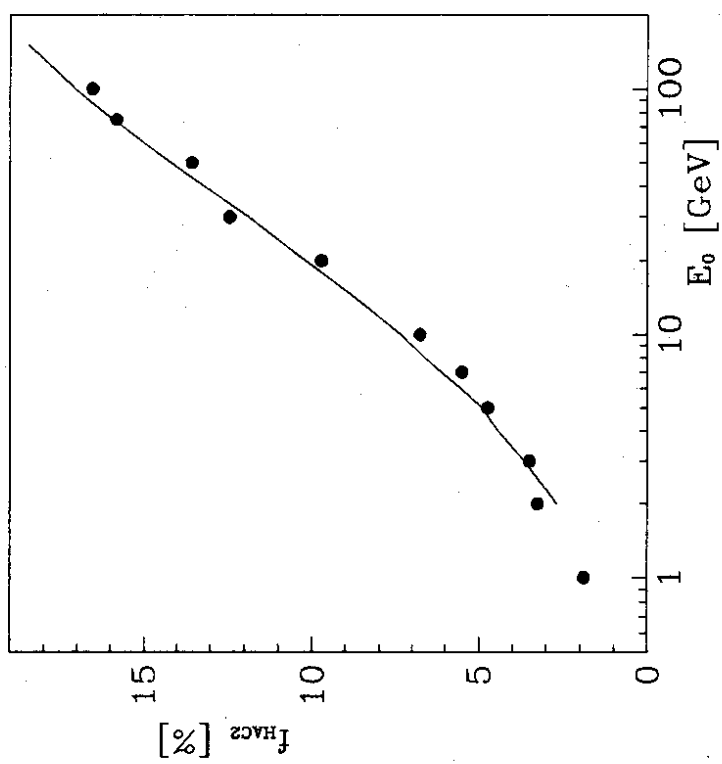


Figure 15: Fraction of energy  $f_{HAC2}$  measured in the HAC2 section of the FCAL prototype, as a function of hadron beam energy  $E_0$ : test data (●) and simulation results (solid line).

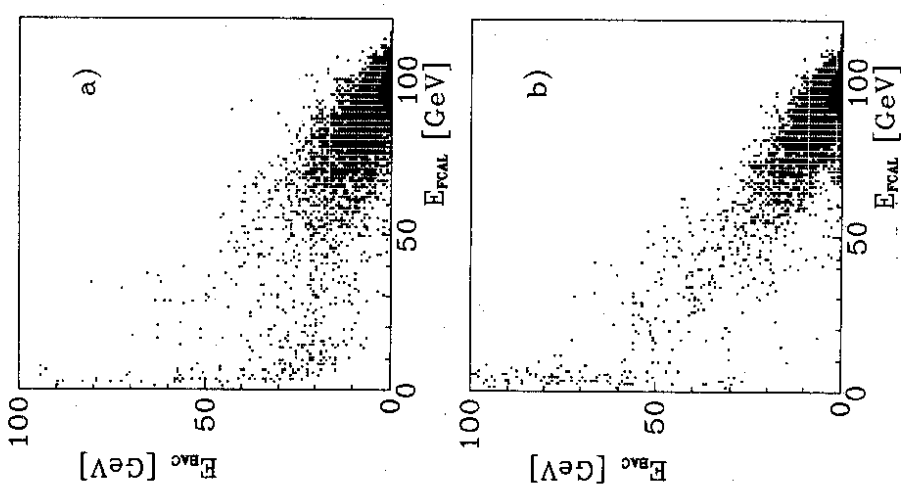


Figure 17: Correlation between the energy measured in the BAC calorimeter -  $E_{BAC}$  and the energy measured in the FCAL calorimeter -  $E_{FCAL}$ , for 100 GeV hadron events, as obtained from the test data (a) and from simulation (b).